Manufacturing PDMS Micro Lens Array using Spin Coating under a Multiphase System

Rongrong Sun, Hanry Yang, D. Mitchell Rock, Roozbeh Danaei, Rahul Panat, Michael R. Kessler, Lei Li*

School of Mechanical and Materials Engineering, Washington State University, Pullman, WA 99164, USA

*E-mail: corresponding author: lei.li2@wsu.edu

Abstract. The development of micro lens arrays has garnered much interest due to increased demand of miniaturized systems. Traditional methods for manufacturing micro lens arrays have several shortcomings. For example, they require expensive facilities and long lead time, and traditional lens materials (i.e. glass) are typically heavy, costly and difficult to manufacture. In this paper, we explore a method for manufacturing a polydimethylsiloxane (PDMS) micro lens array using a simple spin coating technique. The micro lens array, formed under an interfacial tension dominated system, and the influence of material properties and process parameters on the fabricated lens shape are examined. The lenses fabricated using this method show comparable optical properties – including surface finish and image quality – with a reduced cost and manufacturing lead time.

Keywords: micro lens array, spin coating, PDMS.

1. Introduction

As miniaturized systems become more prominent, development of micro lenses and micro lens arrays are needed in various applications; such as, imaging [1], optical sensors (e.g. biosensors [2-3]), 3D endoscopy [4], energy [5], and light coupling [6]. The benefits of miniaturized systems utilizing micro lenses include decreased system size, lower cost, and better portability. These applications have garnered much interest in the past decades as researchers investigated various manufacturing methods, characterization methods, process control approaches, and lens materials in an effort to create and study these systems.

Glass has been a commonly used lens material due to its excellent light transmittance, good environmental and dimensional stability, and high mechanical strength. The studies of glass micro lenses and lens arrays have been conducted for a relatively long time compared to other materials, such as polymeric materials [7]. However, polymeric materials have become a promising alternative for several reasons. One advantage is the density of polymeric material, which is about 2-5 times lower than glass [7]. Another advantage is that polymeric materials are often easy to manufacture, which can greatly decrease the manufacturing cost of micro lenses and lens arrays. Polymeric lenses and lens arrays are typically created using thermoplastic/thermosetting or UV-curable polymers [8-13]. Among polymeric materials, PDMS has attracted significant attention due to its low cost, flexibility, good biocompatibility, ability to be thermally cured or UV cured, and high light transmittance [14]. The transmittance of PDMS is about 85% at the wavelength range of 290-1100nm [15]. Typically, PDMS was used as the mold material in molding process [16-17]. However, PDMS is also a good lens material and the PDMS lens and lens array can be fabricated using replica molding [18-19], printing [13], and femtosecond laser machining [20]. Among all these manufacturing methods, molding method has the advantages of low cost, high production rate and is widely used in industry. However, it requires expensive and sophisticated facilities to make molds, which limits its application in small volume fabrication, especially for customized products. Femtosecond laser scanning is also a rapid manufacturing method, but the surface of the micro lens and lens array is not optically perfect. The printing method, such as drop on demand inkjet printing

method, is a low cost way to generate lenses and lens arrays. However, it is not very suitable to fabricate micro lenses using high viscosity materials such as PDMS. To print high viscosity materials, one can either use a larger printer nozzle, which increases the lens size, or decrease the viscosity by diluting the printing material. Therefore, in this research, we propose a new PDMS micro lens array manufacturing method via a spin coating process.

Spin coating is a procedure widely used in microfabrication to generate uniform thin films on flat substrates. It can be used for coating substrates with various materials such as photoresists, liquid polymers, and many other liquid or sol-gel materials. The film thickness is affected by material properties, spinning speed, and spinning time [21]. It is a useful technique to achieve thin and uniform coating with the advantage of simplicity.

Some processes, such as thermal reflow [8] and molding method [19], also used interfacial tension as auxiliary force to form lenses or molds. Lithography or printing was used to generate a pattern in these methods, and forming lens along with interfacial tension force. These methods can generate micro lenses with good surface finish [8, 19]. Recently, some methods using interfacial tension as the dominant forces to form lenses have been studied to fabricate micro lenses and micro lens arrays [9-10, 15, 22-26]. Such as inkjet printing methods [9, 23-24], and the using of various microfluidic devices [10, 25-26]. Compared to the traditional manufacturing methods, interfacial tension force dominated processes have the advantages of easy fabrication, low cost, good surface finish, and so on. In our previous works, we used interfacial tension force dominated processes to fabricate polymeric biconvex lenses and convex-plano lenses in multiphase systems [9-10]. Ho *et al* presented a lens forming method that utilizes excimer laser microdrilling and spin coating [16, 22]. Their methods can form molds for microlens arrays [16] or self-aligned Poly(methyl methacrylate) (PMMA) double microlens arrays [22] in an interfacial force assisted system. This method does not require direct machining of the complete lens profile which is expensive and time consuming. Instead, they use nature forces, i.e. gravity and surface tension, to generate lens shape and thus is low cost. In this current work, we use interfacial tension as the dominant force in the lens forming process, and studied a manufacturing method to fabricate PDMS micro lens arrays using a spin coating technique under a multiphase system. Surfactants are used to change the substrate's wetting ability, while solvents are used to dilute the PDMS, which changes the rheological properties and surface tension of the coating material. The influence of material properties and process parameters on the final structure of the fabricated micro lenses and lens arrays is examined.

2. Manufacturing process

As discussed above, PDMS is an ideal material for micro lenses due to its good optical properties and low cost. In this research, PDMS micro lens arrays were fabricated using a spin coating procedure. A stainless steel sheet with through holes was used instead of a solid substrate during the spin coating procedure. This perforated sheet plays an important role in the lens forming process, and this substrate also becomes the aperture of the formed micro lens array to block stray light. Figure 1(a), (b) shows the micro lens array manufacturing process. The perforated stainless steel substrate (38.1 mm × 38.1 mm × 0.127 mm) that was cut from a perforated stainless steel sheet (92315T101, McMaster-Carr), was placed on an acrylic holder. The perforations had a 0.1524 mm diameter with a 0.28448 mm center to center distance. The acrylic holder (38.1 mm × 38.1 mm × 3.175 mm) was fabricated using a laser engraver (Speedy300TM, trotec®) to engrave a square pocket of 25.4 mm × 25.4 mm and 1.5 mm deep in the center of the acrylic. The perforated sheet was adhered to the acrylic holder using double sided adhesive tape. Premixed and degassed PDMS (Sylgard® 184 silicone elastomer kit, base and curing agent mixed at a ratio of 10:1, Dow Corning) was deposited on the perforated substrate using a syringe (figure 1(a)). A uniform and thin PDMS layer was obtained after spin coating on a SCK 200 spinner (Intras Scientific) (figure 1(b)). Coating material amount, angular velocity and spin coating time can be used to adjust the film thickness. In this research, we deposited 0.8 ml coating material (PDMS or diluted PDMS in this research) on the perforated steel substrate, and spin coated at 2000 RPM for 30 s. Due to the geometry of

the through holes, capillary force, and gravity, a protuberance was formed in each hole and can be used as a micro lens after curing (figure 1(c)). Because the lens is formed in an interfacial tension dominant system, it can form concave or convex shaped lenses (figure 1(d), (e)) by adjusting the combination of PDMS/steel interfacial tension, PDMS/air interfacial tension and steel/air interfacial tension. In this research, we studied the influence of the substrate pretreatment and coating material (lens material) properties on the lens shape.

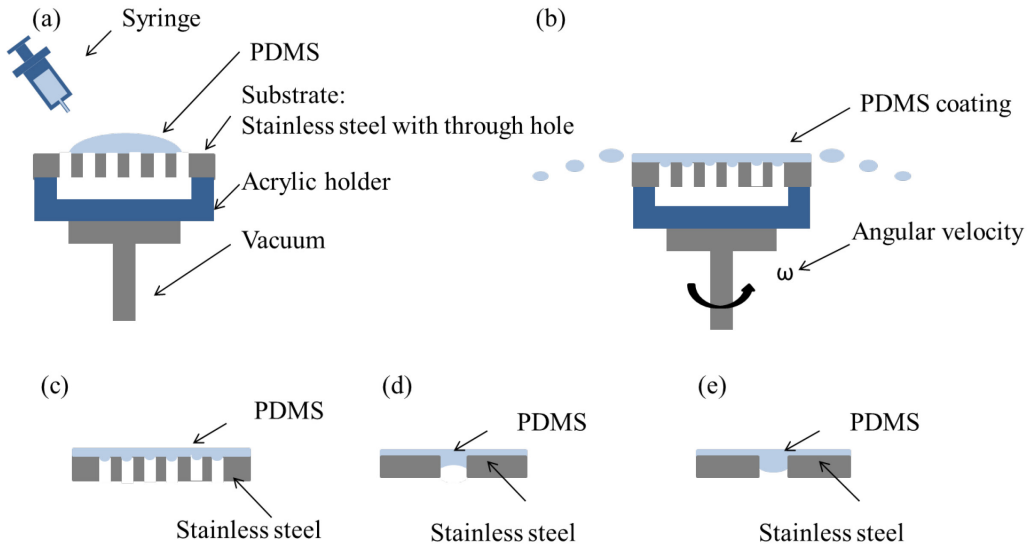

Figure 1. Schematic of the method: (a) applying PDMS; (b) rotating; (c) drying; (d) concave-plano lens; (e) convex-plano lens.

Figure 1(d) shows the schematic of a concave-plano lens. It is a negative lens mainly used for diverging light. The radius of curvature is negative at the concave side and infinite at the plano side. The refractive index of air is approximately 1. By using the assumption of thin lens, the focal length can be calculated using the simplified lens maker's equation, as described by equation 1. This equation is used to calculate the focal length in this study. Figure 1(e) shows the schematic of a convex-plano lens, which is a positive lens that is mainly used for converging lights). The radius of curvature is infinite at the plano side, but it is positive at the convex side.

The focal length (equation 1) is calculated as

$$f = \frac{R_1}{n_{lens}-1} \tag{1}$$

where, f is the focal length; n_{lens} is the refractive index of the lens; R_1 is the radius of curvature on the curved side, which is concave or convex. The profile of the lens was measured using a white light interferometer (NewView 6000, Zygo) and the radius of the lens can be fit using the software Gwyddion (Czech Metrology Institute). The focal length was then calculated using equation 1 with $n_{lens} = 1.4$ for PDMS [27], and also measured using a customized focal length measurement system [10].

2.1. Surface treatment

In this research we studied the influence of substrate surface treatment on the lens shape by varying surfactant (detergent, Dawn) concentration used to treat the perforated sheet, from 0 mL/L to 100 mL/L. The surfactant is a commercial detergent and the main ingredients of the detergent are Sodium Lauryl Sulfate, Sodium Laureth

Sulfate, Lauramine Oxide, PEG-8 Propylheptyl Ether, and PEI-14 PEG-10/PPG-7 Copolymer [28]. To treat the surfaces we first cleaned the perforated sheets in an ultrasonic bath of ethanol for 1 hour, followed by deionized water (DI) washing, and finally drying with pressurized clean air. The cleaned perforated sheets were then immersed in DI water with various surfactant concentrations in an ultrasonic bath for 1 hour and dried at 60 °C for 1 hour. These surfactants coated perforated sheets were used as substrates in the spin coating procedure. After spin coating lens material, samples were directly cured in an oven at 60 °C for 2 hours. To explore the influence of surface treatment on the interfacial tension, contact angle measurements of PDMS droplets on the same stainless steel (without holes) with the same surface treatment were conducted.

Surfactant is expected to change the surface tension of the material. P. Somasundaran *et al*. have conducted some research on the influence of surfactant on the wettability of solid substrates, such as alumina. Their study showed that without surfactant, alumina exhibits hydrophilicity. As the concentration of surfactant increased, the alumina began to show hydrophobicity, as indicated in Figure 2 [29]. In this study, we pre-coated different amounts of surfactant on the stainless steel. The changing hydrophobicity of the coated perforated steel surface will affect the interfacial tension, which can be observed by the change in contact angle. The interfacial tension will also impact the final shape of the lens. More detail about surface treatment mechanism is a topic of interest for future studies.

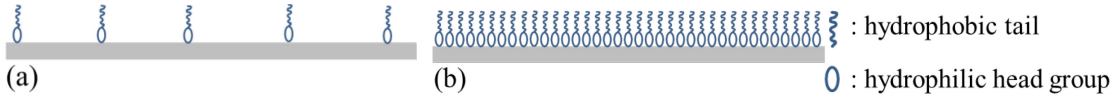

Figure 2. Mechanism of surface treatment.

2.2. Material properties

Besides surface treatment, the properties of the coating material will also affect the lens shape. To investigate the influence of the coating material, we diluted PDMS using hexanes (Reagent Grade, VWR) to obtain different coating material properties, i.e. surface tension and viscosity. The concentration of diluted PDMS solution varied from 30% to 100%. To measure the contact angle, the diluted PDMS droplet was deposited on plain sheets (without holes) of the same stainless steel material. Contact angles of materials with different PDMS concentrations to substrates were measured and compared. The viscosity of the diluted PDMS was measured using an ARES G2 strain-controlled rheometer (TA Instruments). Steady state viscosity data was collected at room temperature over the shear rate range 10 to 100 s^{-1} using recessed concentric cylinder geometry (cup diameter 29.987 mm, bob diameter 27.665 mm). The material was sheared for 30 s at each specified shear rate then data was collected and averaged over 10 s to give a viscosity value for each point. The thickness of the thin film on the unperforated steel sheet was measured using a profilometer (DektakXT, Bruker). The profilometer has a stylus with a radius of 12.5 µm. Data was collected in the range of 6.5 µm. The speed of measurements was 10 µm/s and stylus force was adjusted to 0.1 mg. The reported thickness is the average of three measurements.

3. Results and Discussion

3.1. Effects of surface treatment

3.1.1. Effects of surface treatment to wettability. To investigate the influence of surfactant concentration on the film thickness, we spin coated a thin film on unperforated stainless steel substrates. Figure 3 shows the relationship between film thickness and surfactant concentration. The error bars represent the standard deviation of samples. The data in figure 3 indicate that the thickness remains relatively constant as the surfactant concentration increases.

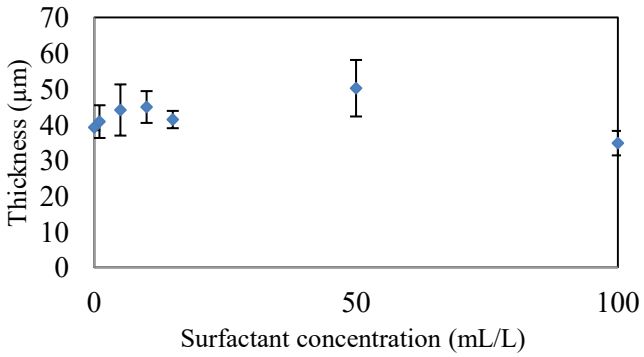

Figure 3. Thickness vs surfactant concentration.

Figure 4 shows the relationship between contact angle and surfactant concentration. The fitting curve shows the trend of the change. At low surfactant concentrations, the contact angle increases with the increasing of surfactant concentration. However, when surfactant concentration is larger than 15 mL/L, the contact angle increases slowly and reach the maximum around 100 mL/L. It indicates the substrate reaches the maximum hydrophobicity, which shows similar tendency of P. Somasundaran's research [29]. The inserted images are the side views of the PDMS droplet on the substrate during the contact angle measurement. The left image is the experimental image of contact angle when surfactant concentration is 1 mL/L, while the right image is the one when surfactant concentration is 100 mL/L. This change of wettability and contact angle will affect the lens shape in the lens array manufacturing process.

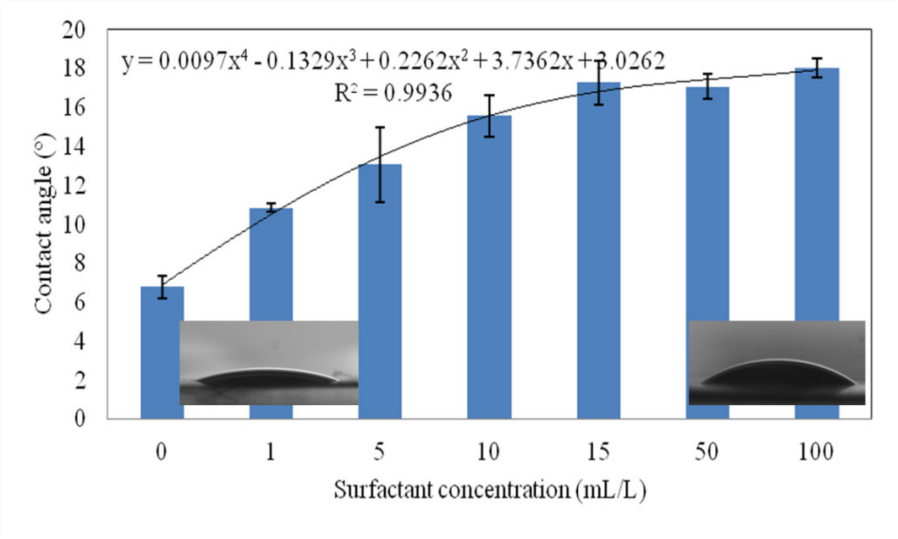

Figure 4. Contact angle vs surfactant concentration.

3.1.2. Effects of surface treatment on the lens shape and focal length. In this research, we pretreated the perforated sheet using different surfactant concentrations and spin coated a PDMS thin film on the pretreated sheet. Figure 5(a) shows the relationship between radius of curvature and surfactant concentration. The radius of curvature for low surfactant concentration (0 mL/L and 1 mL/L) is very large, indicating that the lens surfaces are nearly flat under these two conditions. As the surfactant concentration changes from 5 mL/L to 100 mL/L, the radius of curvature decreases. It decreases quickly when the concentration is less than 15 mL/L, and slow down after that. The change in lens shape and decreasing radius of curvature is attributed to the change in PDMS wettability to substrates caused by the varying surfactant concentration pretreatment. For the 0 mL/L surfactant solution, no surfactant molecules were

coated on the steel surface. The substrate shows hydrophilicity and concave shaped lenses (negative radius of curvature, near to a parallel plate) were formed in the micro holes. With the increase of surfactant concentration, surfactant molecules start to attach to the substrate and the substrate begins to show hydrophobicity. The change in surfactant molecular coverage affects the surface wettability and changes the contact angle of the material on the substrate, resulting in different lens shapes. Using equation 1, we can calculate the focal length using the measured radius of curvature. The results are shown in figure 5(b), blue data (columns with dashed line fillings). The red solid data shown in figure 5(b) are experimental results. When the surfactant concentration is small (less than 7mL/L), the radius of curvature is very large, and the formed lens is close to flat plate rather than microlens. Moreover, when radius of curvature of the lens is large, the curvature of the other surface (which we assumed as flat surface) begins to show influence. Therefore, we only consider lenses formed with surfactant concentration above 7 mL/L. Figure 5(b) shows the comparison from 7 mL/L to 100 mL/L. The value calculated using equation 1 is close to the measured value. The difference between them came from assumptions of equation 1 and measurement errors. From the calculated data in figure 5(b), the focal length changes from around 0.3 mm to around 5 mm in this region.

Figure 6 shows three typical cross section profiles of the lenses. When the substrate is pretreated with 0 mL/L surfactant solution (the red line in figure 6), the formed lens shape was close to flat. With the increase of the surfactant concentration, the lens shape changed to convex. When the surfactant concentration was low (the blue line in figure 6), the radius of curvature is comparably large. With continue increasing surfactant concentration the lens became more protruded (the black line in figure 6). This figure shows that lenses change from plano-plano to convex-plano shape (converging lens). Due to the limitation of white light interferometer, steep curves cannot be measured. Some portion of the lens profile, especially at steep edges, cannot be seen. Dashed lines were used in figure 6 (and figure 11) to indicate the relative distance from the lens profile to the face of perforated sheet.

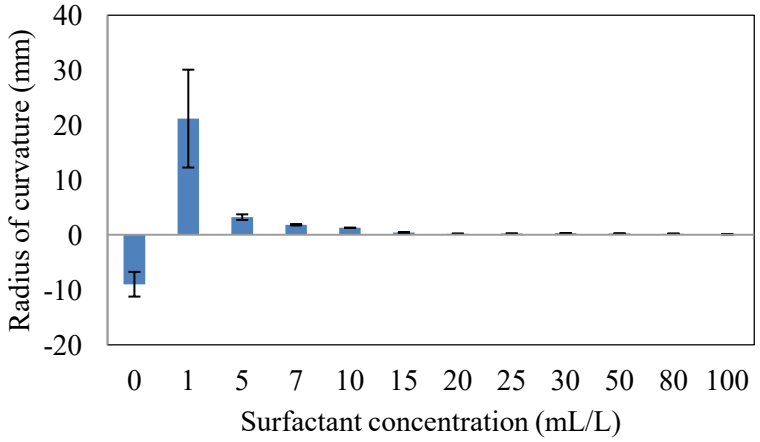

(a) Relationship between radius of curvature and surfactant concentration (negative radius of curvature represents concave lens, vice versa).

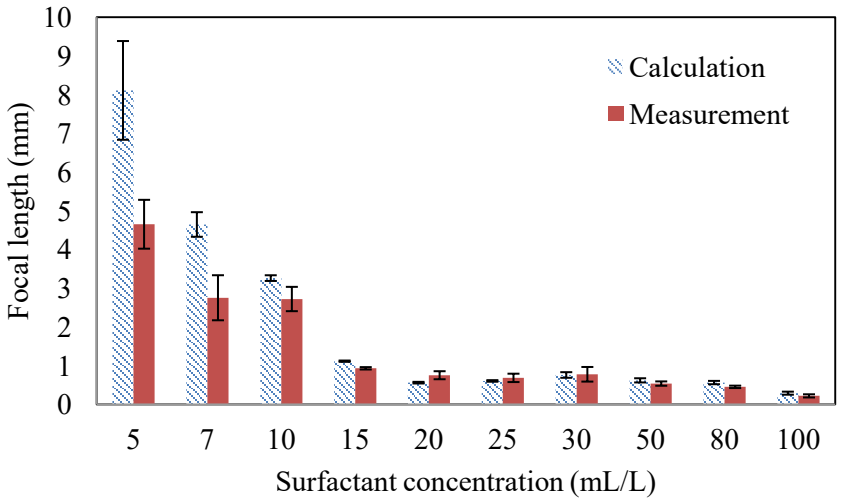

(b) Relationship between focal length and surfactant concentration.

Figure 5. Influence of the surfactant concentration.

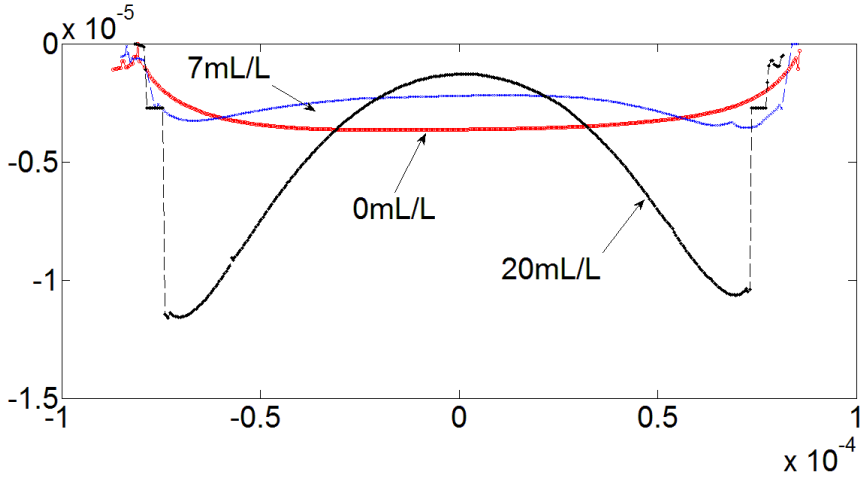

Figure 6. Lens shape at different surfactant concentration (unit, m).

3.2. Effects of Materials properties

3.2.1. Materials property characterization. To change the material properties, like viscosity and surface tension, we diluted PDMS using hexanes. To avoid the influence of material curing, we only used neat PDMS resin in the viscosity measurements (no curing agent was used). The normalized viscosities of the diluted PDMS solutions were measured and the results were plotted in figure 7. Since the viscosity of hexanes is much lower than pure PDMS, the presence of hexanes, decreases the viscosity of diluted PDMS. Figure 7 shows that when the PDMS concentration is less than 70%, the normalized viscosity is low, after that, the normalized viscosity increases rapidly, especially from 90% to 100%.

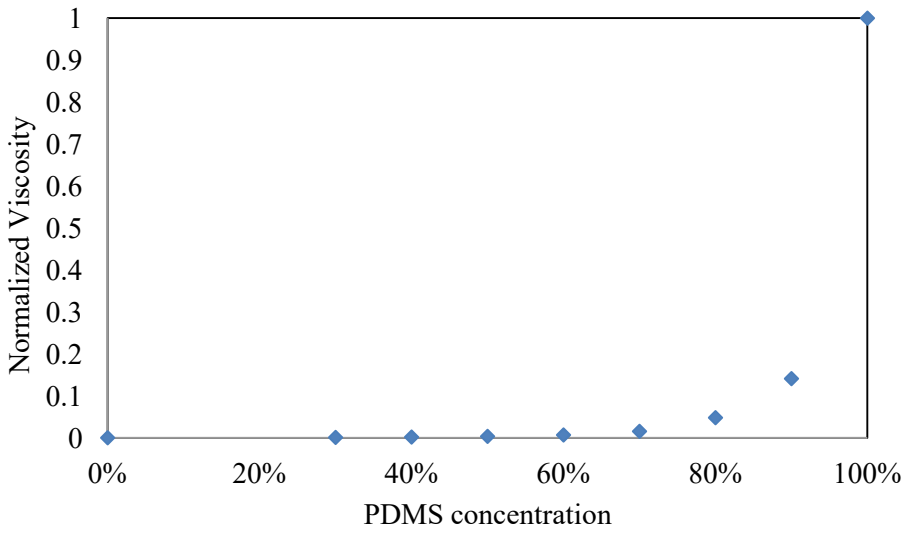

Figure 7. Normalized viscosity changes with PDMS concentration in hexanes.

Figure 8 shows the relationship between film thickness and the hexanes-diluted PDMS concentration with both bare stainless sheet and pretreated sheet. When we increased PDMS concentration, the solution's viscosity increased, resulting in a thicker film on the substrate after the spin coating process. When the concentration is lower than 30%, it is difficult to form lenses on the perforated stainless steel sheet, and difficult to measure the thickness on the solid substrate using the profilometer. This figure indicates that the viscosity of the lens material has a strong effect on the film thickness. By comparing the bare substrate data (blue columns with dashed line fillings) to the pretreated substrate data (red solid columns), similar trends are observed and the film thicknesses of both conditions increased with increasing of PDMS concentration. This figure indicates that the viscosity of the coating material has a larger impact on thickness than the pretreatment process.

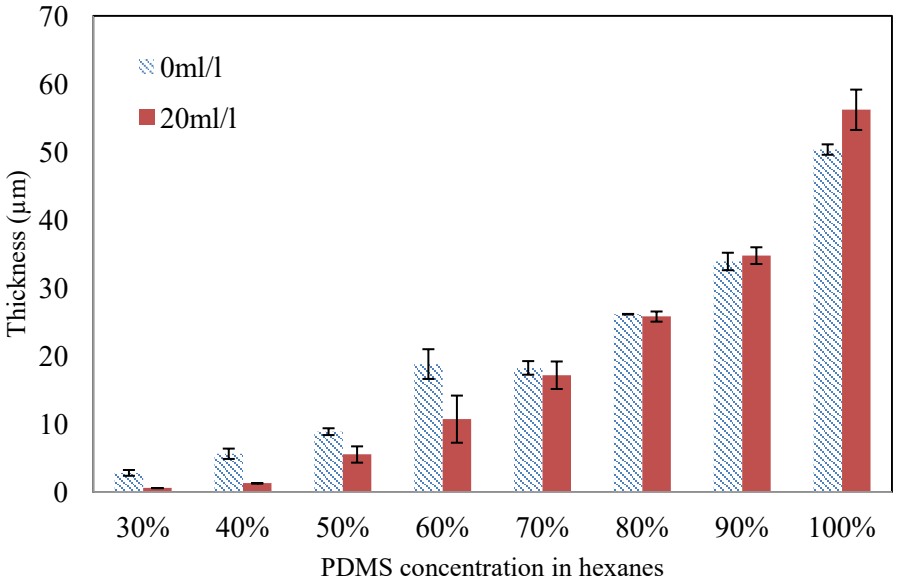

Figure 8. Relationship between thickness and PDMS concentration.

Contact angles of the diluted PDMS to the bare stainless steel sheets and pretreated stainless steels were measured and plotted in figure 9. Due to the presence of hexanes, the diluted PDMS has a smaller contact angle with the substrate compared to pure PDMS (100%). With the decrease of PDMS concentration from 100% to 40%, the contact angle decreased from 16.9 º to 10.7 º on the pretreated substrate, and decreased from 11.8 º to 5.4 º on the bare substrate. Contact angles of 30% samples were too small to measure. By comparing the red solid data (using the pretreated substrate) with the blue data (columns with dashed line fillings, using the bare substrate), it can be seen that the surfactant pretreatment increased the contact angle, meaning the substrate becomes more hydrophobic after pretreatment.

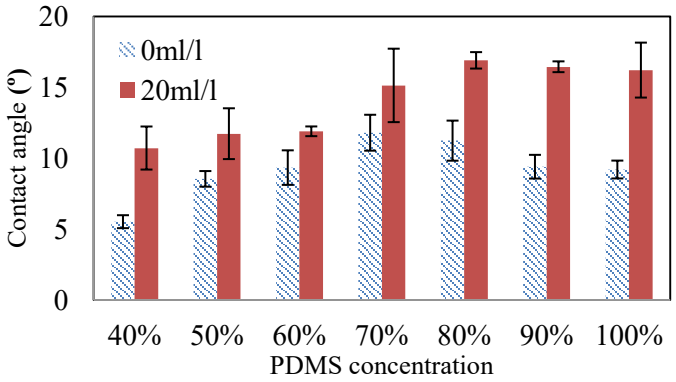

Figure 9. Contact angle changes with PDMS concentration in hexanes.

3.2.2. Effects of material property on lens shape and focal length. In this section, we used diluted PDMS as a coating material. We used bare perforated stainless steel sheets, and pretreated (using 20mL/L surfactant concentration) perforated stainless steel sheets as substrates. The results are plotted in figure 10. Figure 10(a) shows the case when the PDMS concentration is less than 70%, the radius of curvature is negative and therefore the lens shape is concave. The absolute value of radius of curvature increased with the increases of PDMS concentration when the concentration is less than 70%. Comparing the results from substrates with and without pretreatment (red solid columns and blue columns with dashed line fillings in figure 10) shows that the radius from bare substrates is slightly larger than that of the pretreated substrates. In this lens forming process, we could not form lens when PDMS concentration was 30% with bare substrates; however, it worked when we use pretreated substrates. Again, this indicates that the pretreatment process changed the wettability of the coating material to the substrate. When the PDMS concentration is equal or larger than 70%, the radius of curvature is positive. For the lenses which were formed on the bare substrates, lenses radii were larger than 7 mm, meaning the curves were close to flat (the different sign of radius of curvature at figure 5(a) and figure 10(a) with pure PDMS, bare substrate is due to the fit error, since both of them indicate that the curves are close to flat). For lenses formed on pretreated substrates, all the radii were less than 5 mm, and decreased with increasing PDMS concentration. Figure 10(b) shows the focal lengths of manufactured lenses with different PDMS concentration. Since most of lenses formed on bare substrates were very flat, we only compare the lenses formed on the pretreated substrate in figure 10(b). Blue data (columns with dashed line fillings) represents the calculated results while the red solid data denotes the measured results. The results are similar to each other except the data when PDMS concentration is 70%. The calculated focal length was based on the assumption that one side of the lens is flat and the other side has a radius of curvature, and the thickness of the lens was also neglected. However, in reality the other side of the lens is not absolute flat (due to surface tension) and the thickness of the lens also has influence. For the 70% PDMS case, the curved side has a large radius of curvature, which made the flat side curvature and lens thickness more influential and thus there is a large difference between measurement result and calculation result. When we only considering one curved side, the calculated focal lengths for 60%, 70% and 80% PDMS concentrations is -0.48 mm, 12.13 mm, and 2.82 mm, respectively. If we take the radius of curvature of ‘plano side’ into

account, the calculated focal lengths become -0.21mm, 4.06 mm, 1.61 mm, which agreed with the measured focal lengths better (-0.19 mm, 2.12 mm, and 1.06 mm). Therefore, the focal length of the fabricated lens can be well calculated using equation 1 only when the radius of curvature of the curved side is small. The effect of the 'plano side' needs to be considered when the radius of curvature of the curved side is comparably large. The calculated data in this research shows that the focal lengths changed from 0.25 mm to 4.06 mm, and the lens converted from divergence lens to convergence lens.

Figure 11 shows the typical profiles of lenses formed at different forming conditions. Figure 11(a) shows the lenses formed on bare substrates. When PDMS concentrations were 70% and 100%, the lenses were flat (the black and green lines in figure 11(a)). When PDMS concentrations were 60% and 40%, concave shapes were formed (the blue and red lines in figure 11(a)). Figure 11(b) shows the lenses formed on pretreated substrates. When the PDMS concentration was 100% (the green line in figure 11(b)), the lens shape was convex, which is different compared to the one formed on bare substrate. When the PDMS concentration was 70% (the black line in figure 11(b)), the lens shape was close to flat. When the PDMS concentrations were 60% and 40% (the blue and red lines in figure 11(b)), the shapes were concave.

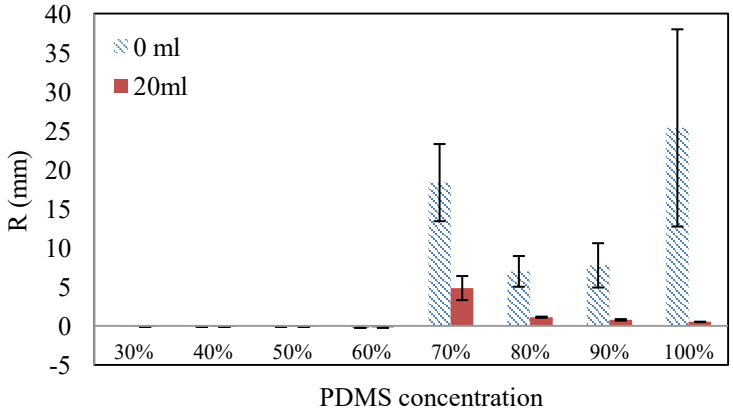

(a) Radius of curvature changes with PDMS concentration in hexanes.

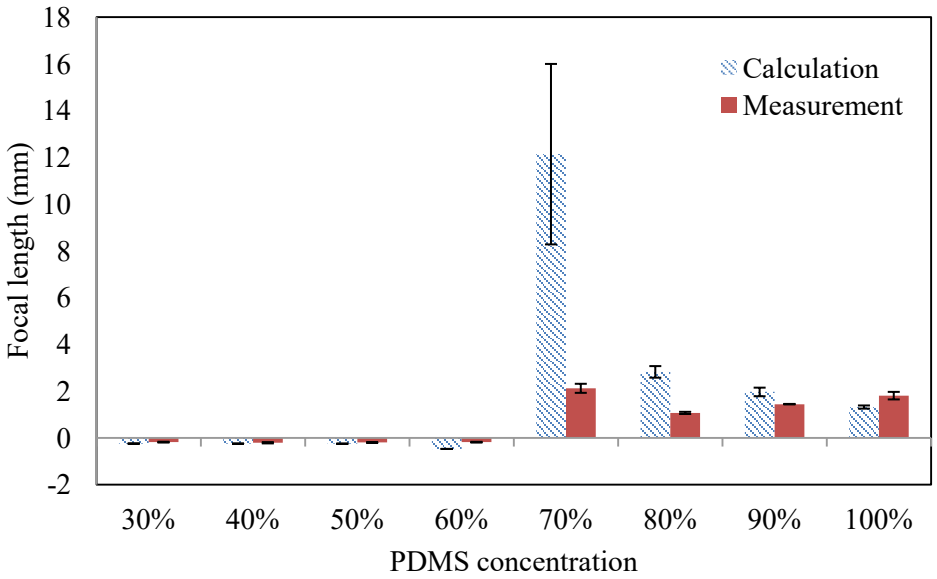

(b) Focal length changes with PDMS concentration (pretreated substrate).

Figure 10**.** Influence of PDMS concentration.

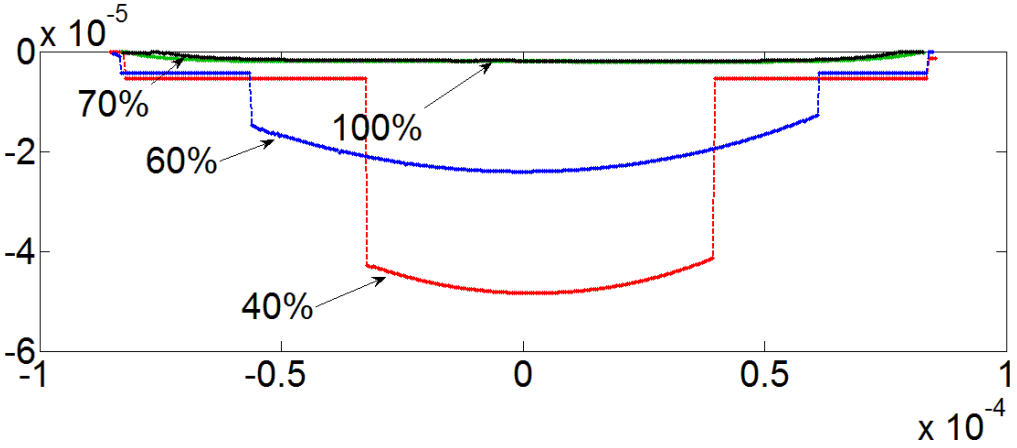

(a) DI.

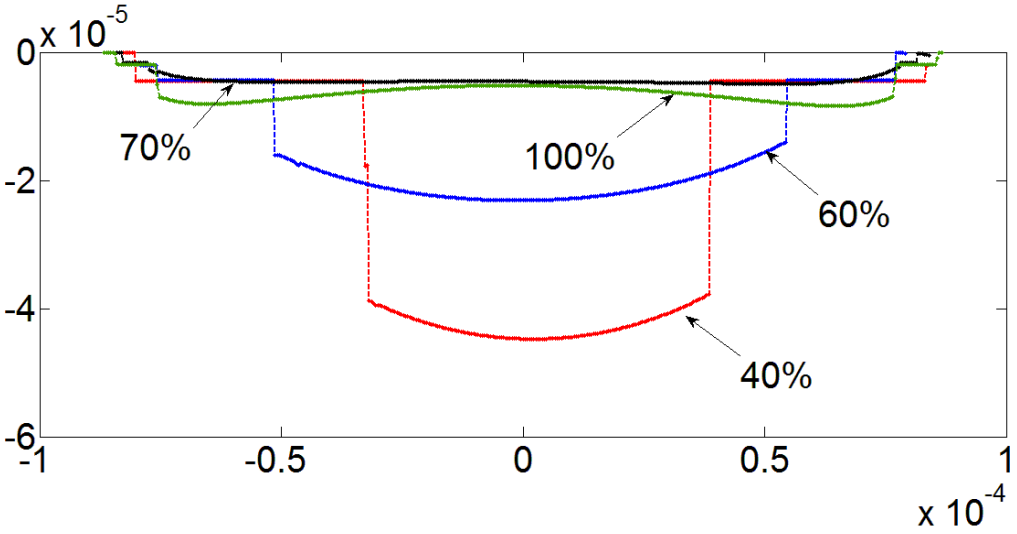

(b) 20mL/L.

Figure 11. Lens shape at different PDMS concentration in hexanes (unit, m).

3.3 Optical properties

Surface roughness is one of the most important properties for an optical lens. A rough surface will scatter light. We measured lens surface roughness by using a white light interferometer. The results indicated that the roughness Ra is 40 nm on average (figure 12(a)). We also used a compound microscope (Zeiss Axio Scope A1) with 20X magnification to take an image of the stainless steel perforated sheet (as shown in figure 12(b)), it indicates that the sheet has uniform holes with smooth edges.

Figure 13(a), (b) are images of lenses which were formed using 100% PDMS in hexanes and 40% PDMS in hexanes on pretreated substrate. The object distance and the object size in figure 13(a) is 490 mm and 5.9 mm ×5.9 mm, respectively. The object distance and the object size in figure 13(b) are 220 mm and 11.8 mm ×11.8 mm, respectively. Figure 13(c) shows the larger images of figure 13(b) using larger magnification. The insert shows the Washington State University logo which is used as the object. Figure

13(d) shows the image of a PDMS micro lens array (peeled off from the template) taken by a compound microscope with 10X magnification, and it shows that the lenses are uniform. Figure 14 shows the point spread function (PSF) of the fabricated lens array (with 40% PDMS, 20 mL/L pretreatment) by using a He-Ne laser and a 25µm aperture as the point light source. Figure 14(a) shows the result using 2.4X magnification, while figure 14(b) shows the result using 4X magnification. From figure 14(b) it can be seen that the incident laser beam was focused to an array of spots with an average spot size 21µm (the first order dark ring).

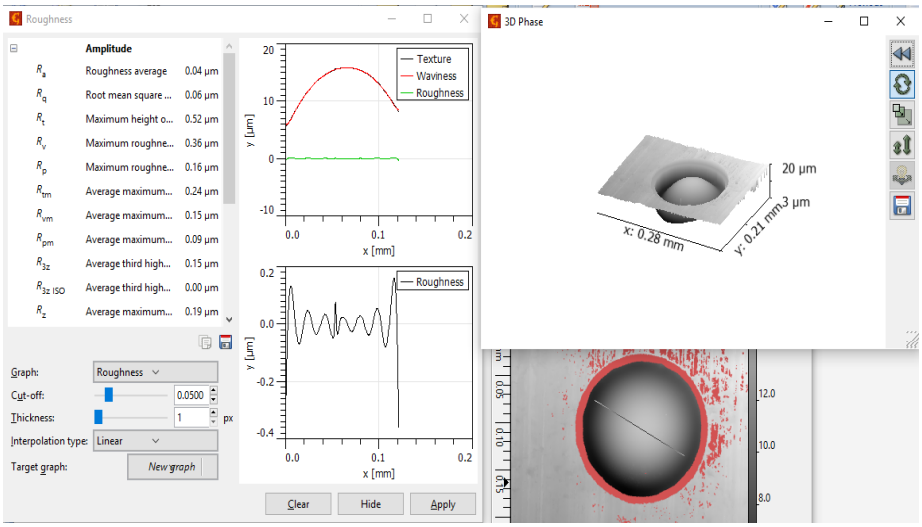

(a) Surface roughness of the fabricated lens

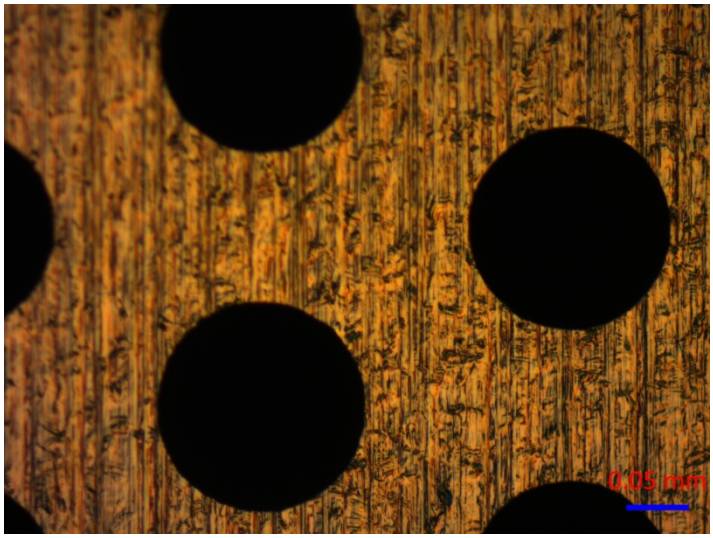

(b) image of the perforated sheet

Figure 12**.** Surface roughness.

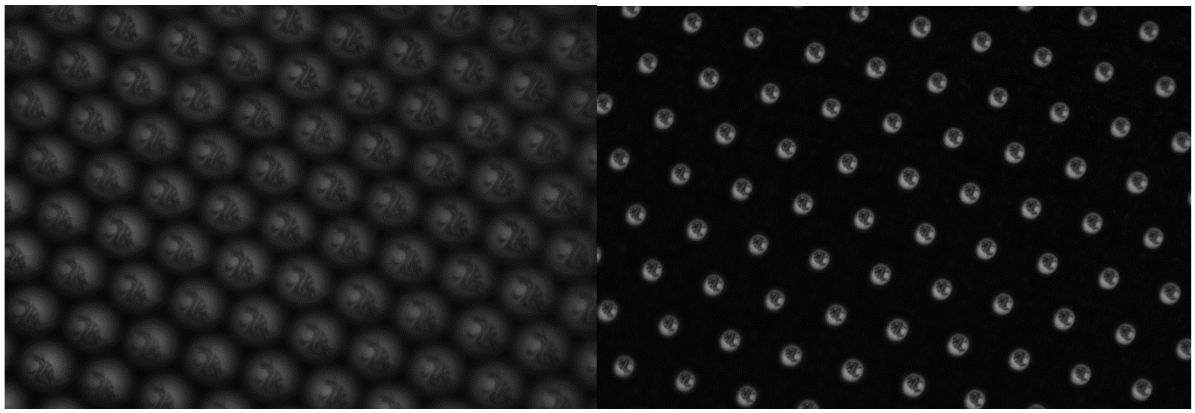

(a) Pure PDMS. (b) 40% PDMS.

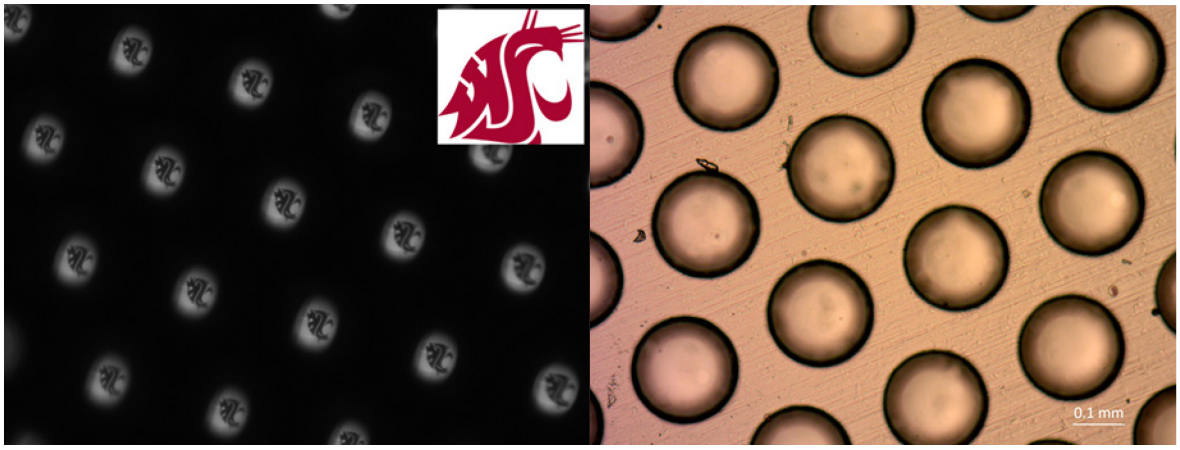

(c) 40% PDMS. (d) Image of the fabricated micro lens array (peeled off from stainless substrate).

Figure 13**.** Images of lens array at different forming conditions.

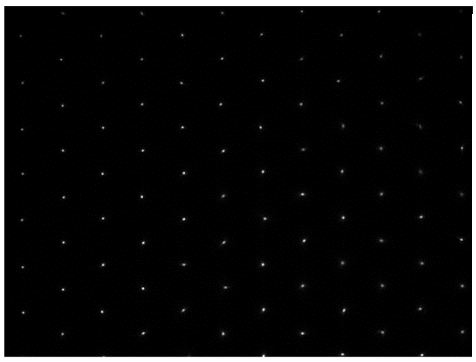

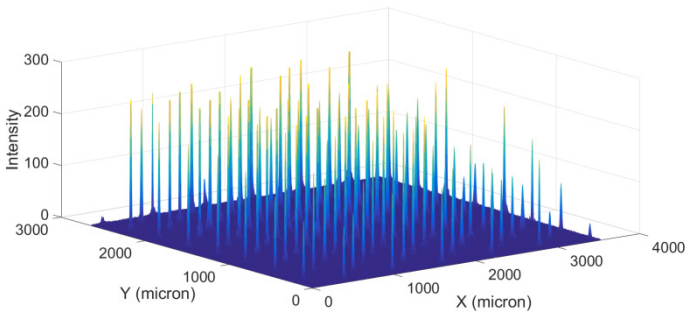

(a) 2.4X magnification.

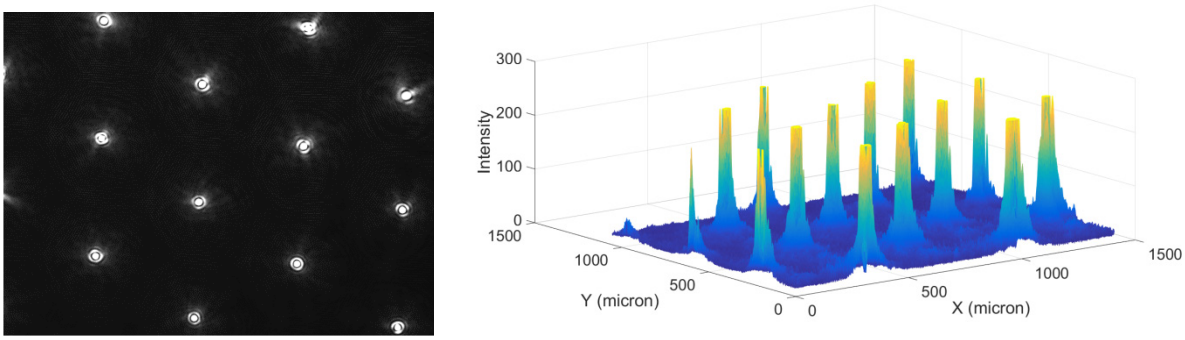

(b) 4X magnification.

Figure 14. Point spread function of lens array.

4. Conclusion

In this study, we demonstrated a PDMS micro lens array manufacturing method by using a spin coating process in a multiphase system. Concave-plano micro lens arrays and convex-plano micro lens arrays can be obtained by pretreating perforated sheets or by using diluted PDMS. The relationship between focal length and surfactant concentration was studied. This research also indicated that the changes of coating material properties, including viscosity and surface tension, would change the lens shape (from concave-plano to convex-plano). Optical properties of PDMS micro lens arrays were demonstrated in this paper. It shows PDMS micro lenses fabricated using this method have good optical properties and can be used for imaging applications.

Acknowledgements

The authors are grateful for the financial support from the National Science Foundation (Grant No. CMMI-1538439). The authors would also like to thank Dr. Indranath Dutta for helping with the white light interferometer. And thank the Frank Innovation Zone of Washington State University for help with their laser engraver.

Reference

[1] X. Jin, D. Guerrero, R. Klukas, and J. F. Holzman 2014 Microlenses with tuned focal characteristics for optical wireless imaging *Appl. Phys. Lett.*, vol. 105, p. 031102.

[2] L.-J. Wang, R. Sun, T. Vasile, Y.-C. Chang, and L. Li 2016 High-Throughput Optical Sensing Immunoassays on Smartphone *Anal. Chem.*, vol. 88, pp. 8302–8308.

[3] L.-J. Wang, Y.-C. Chang, R. Sun, and L. Li 2017 A multichannel smartphone optical biosensor for high-throughput point-of-care diagnostics *Biosens. Bioelectron.*, vol. 87, pp. 686–692.

[4] A. Hassanfiroozi, Y.-P. Huang, B. Javidi, and H.-P. D. Shieh 2015 Hexagonal liquid crystal lens array for 3D endoscopy *Opt. Express*, vol. 23, pp. 971–981.

[5] X. Xiao, Z. Zhang, S. Xie, Y. Liu, D. Hu, and J. Du 2015 Enhancing light harvesting of organic solar cells by using hybrid microlenses *Opt. Appl.*, vol. 45, pp. 89-100.

[6] M. Zaboub, A. Guessoum, N.-E. Demagh, and A. Guermat 2016 Fabrication of polymer microlenses on single mode optical fibers for light coupling *Opt. Commun.*, vol. 366, pp. 122–126.

[7] H. Ottevaere *et al.* 2006 Comparing glass and plastic refractive microlenses fabricated with different technologies *J. Opt. Pure Appl. Opt.*, vol. 8, p. S407.

[8] H. Yang, C.-K. Chao, M.-K. Wei, and C.-P. Lin 2004 High fill-factor microlens array mold insert fabrication using a thermal reflow process *J. Micromechanics Microengineering*, vol. 14, p. 1197.

[9] R. Sun, Y. Li, and L. Li 2014 Rapid method for fabricating polymeric biconvex parabolic lenslets *Opt. Lett.*, vol. 39, p. 5391.
[10] R. Sun, L. Chang, and L. Li 2015 Manufacturing polymeric micro lenses and self-organised micro lens arrays by using microfluidic dispensers *J. Micromechanics Microengineering*, vol. 25, p. 115012.
[11] L.-J. Lai, H. Zhou, and L.-M. Zhu 2016 Fabrication of microlens array on silicon surface using electrochemical wet stamping technique *Appl. Surf. Sci.*, vol. 364, pp. 442–445.
[12] C. Florian, S. Piazza, A. Diaspro, P. Serra, and M. Duocastella 2016 Direct Laser Printing of Tailored Polymeric Microlenses *ACS Appl. Mater. Interfaces*, vol. 8, pp. 17028–17032.
[13] S. Damodara, D. George, and A. K. Sen 2016 Single step fabrication and characterization of PDMS micro lens and its use in optocapillary flow manipulation *Sens. Actuators B Chem.*, vol. 227, pp. 383–392.
[14] R. Mukhopadhyay 2007 When PDMS isn't the best *Anal. Chem.*, vol. 79, pp. 3248–3253.
[15] T.-K. Shih, C.-F. Chen, J.-R. Ho, and F.-T. Chuang 2006 Fabrication of PDMS (polydimethylsiloxane) microlens and diffuser using replica molding *Microelectron. Eng.*, vol. 83, pp. 2499–2503.
[16] T.-K. Shin, J.-R. Ho, and J. W. J. Cheng 2004 A new approach to polymeric microlens array fabrication using soft replica molding *IEEE Photonics Technol. Lett.*, vol. 16, pp. 2078–2080.
[17] X. Zhu, L. Zhu, H. Chen, L. Yang, and W. Zhang 2016 Micro-ball lens structure fabrication based on drop on demand printing the liquid mold *Appl. Surf. Sci.*, vol. 361, pp. 80–89.
[18] S. Park *et al.* 2006 Fabricaton of Poly(dimethylsiloxane) Microlens for Laser-Induced Fluorescence Detection *Jpn. J. Appl. Phys.*, vol. 45, p. 5614.
[19] X. Ke *et al.* 2012 Fabrication of poly(dimethylsiloxane) concave microlens arrays by selective wetting and replica moulding *Micro Amp Nano Lett.*, vol. 7, pp. 1121–1124.
[20] J. Yong *et al.* 2013 Rapid Fabrication of Large-Area Concave Microlens Arrays on PDMS by a Femtosecond Laser *ACS Appl. Mater. Interfaces*, vol. 5, pp. 9382–9385.
[21] J. H. Koschwanez, R. H. Carlson, and D. R. Meldrum 2009 Thin PDMS Films Using Long Spin Times or Tert-Butyl Alcohol as a Solvent *PLOS ONE*, vol. 4, p. e4572.
[22] J.-R. Ho, T.-K. Shih, J.-W. J. Cheng, C.-K. Sung, and C.-F. Chen 2007 A novel method for fabrication of self-aligned double microlens arrays *Sens. Actuators Phys.*, vol. 135, pp. 465–471.
[23] W.-C. Chen, T.-J. Wu, W.-J. Wu, and G.-D. J. Su 2013 Fabrication of inkjet-printed SU-8 photoresist microlenses using hydrophilic confinement *J. Micromechanics Microengineering*, vol. 23, p. 065008.
[24] D. Xie, H. Zhang, X. Shu, and J. Xiao 2012 Fabrication of polymer micro-lens array with pneumatically diaphragm-driven drop-on-demand inkjet technology *Opt. Express*, vol. 20, pp. 15186–15195.
[25] T. Nisisako 2016 Recent advances in microfluidic production of Janus droplets and particles *Curr. Opin. Colloid Interface Sci.*, vol. 25, pp. 1–12.
[26] T. Nisisako, T. Ando, and T. Hatsuzawa 2014 Capillary-Assisted Fabrication of Biconcave Polymeric Microlenses from Microfluidic Ternary Emulsion Droplets *Small*, vol. 10, pp. 5116–5125.
[27] Sylgard®184 Silicone Elastomer 2014 Dow Corning and Sylgard are registered trademark s of Dow Corning Corporation, 11-3184-01.
[28] P&G, Ultra Dawn® Product safety and ingredients datasheet, https://www.pg.com/productsafety/ingredients/household_care/dish_washing/Dawn/Ultra_Dawn_Hand_Renewal.pdf.
[29] P. Somasundaran and L. Zhang 2006 Adsorption of surfactants on minerals for wettability control in improved oil recovery processes *J. Pet. Sci. Eng.*, vol. 52, pp. 198–212.